SIAM J. APPL. MATH.
Vol. 38, No. 3, June 1980


0036-1399/80/3803-0003 $01.00/0

# REACTIVE-DIFFUSIVE SYSTEM WITH ARRHENIUS KINETICS: PECULIARITIES OF THE SPHERICAL GEOMETRY*

A. K. KAPILA,† B. J. MATKOWSKY‡ AND J. VEGA¶

**Abstract.** The steady reactive-diffusive problem for a nonisothermal permeable pellet with first-order Arrhenius kinetics is studied. In the large activation-energy limit, asymptotic solutions are derived for the spherical geometry. The solutions exhibit multiplicity, and it is shown that a suitable choice of parameters can lead to an arbitrarily large number of solutions, thereby confirming a conjecture based upon past computational experiments. Explicit analytical expressions are given for the multiplicity bounds (ignition and extinction limits). The asymptotic results compare very well with those obtained numerically, even for moderate values of the activation energy.

**1. Introduction.** This paper treats the Dirichlet problem for a nonisothermal permeable catalyst pellet with first-order Arrhenius kinetics. The governing equation is

$$\nabla^2 y = -\lambda^2(1+\beta-y)\exp[\gamma(y-1)/y] \quad \text{in } \Omega \tag{1.1a}$$

with boundary condition

$$y = 1 \quad \text{on } \partial\Omega. \tag{1.1b}$$

Here $\Omega$ is the region interior to the pellet and $\partial\Omega$ its external surface, $y$ is the temperature of the reacting species, and the nonnegative parameters $\beta$, $\gamma$ and $\lambda$ are, respectively, the chemical heat release, the activation energy of the reaction and the Thiele modulus. The variables have been suitably nondimensionalized.

An extensive discussion of the background of the problem has been given by Aris [1]. Summarizing briefly, it is known that if $\gamma$ is large enough, there exist constants $\lambda_0$ and $\lambda^0$, depending upon $\beta$, $\gamma$ and the domain $\Omega$, such that (1.1) has multiple solutions for $\lambda_0 \leqq \lambda \leqq \lambda^0$. These solutions are displayed conveniently on the so-called response diagram, which is a graph of the maximum value of $y(x)$ against $\lambda$ for fixed $\beta$ and $\gamma$. For the one-dimensional slab and the cylindrically symmetric geometries the response is known to be $S$-shaped (see curve (a) in Fig. 1), indicating that there can be one, two or three solutions. For the spherically symmetric geometry, computational results [2]–[4] suggest that the number of solutions may be very large, perhaps even arbitrarily so, for certain parameter values. It is conjectured that the response then has the shape of curve (b) in Fig. 1.

The object of this paper is to demonstrate the truth of the above conjecture. This is done by obtaining asymptotic expansions of the solutions of (1.1) for the spherically symmetric geometry in the limit of large activation energy ($\gamma \to \infty$). The procedure leads to an analytical description of the *entire* response curve, and also yields explicit asymptotic expressions for the multiplicity bounds $\lambda_0$ and $\lambda^0$. These asymptotic values are shown to be in good agreement with numerical results.

A similar analysis for the slab and cylindrical geometries was carried out by Kapila and Matkowsky in a recent paper [5]. Familiarity with [5] will be helpful to the reader,

* Received by the editors October 24, 1978, and in revised form May 31, 1979. This research was partially supported by the United States Army Research Office under Grants DAAG 29-76-G-0253, DAAG 29-76-G-0315 and DAAG 29-77-6-0222, by the National Science Foundation under Grant MCS77-25660, and by the Department of Energy under Grant ER 78-S-02-4650.

† Department of Mathematical Sciences, Rensselaer Polytechnic Institute, Troy, New York 12181.

‡ Department of Engineering Sciences and Applied Mathematics, Evanston, Illinois 60201.

¶ Escuela Tecnica Superior de Ingenieros Aeronauticos, Universidad Politechnica de Madrid, Madrid 3, Spain.

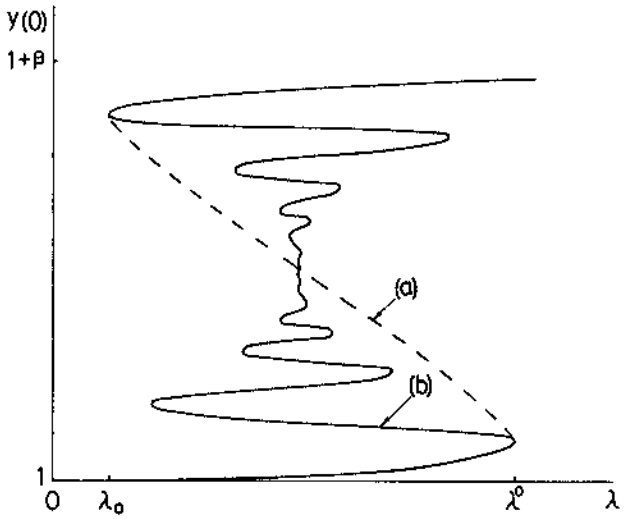


FIG. 1. *The response curve [graph of Thiele modulus λ against maximum temperature y(0)] for* (a) *slab and cylinder,* (b) *sphere.*

since most of the notation employed there is retained here. However, the present paper is self-contained, and even though some of the analysis carries over from [5], for the most part the spherical geometry displays a peculiarity of its own. The physical reason for this peculiarity is not clear; perhaps it is a characteristic of bounded domains $\Omega$. It is worth pointing out that at least for unit Lewis number (the ratio of material to thermal diffusivity) only the highest and the lowest branches of the response curves (a) and (b) of Fig. 1 are stable (see Jackson [6]). In that respect, therefore, there is little qualitative difference between the sphere and the other two geometries.

A leading-order asymptotic description of the extreme branches of curve (a) of Fig. 1 was given independently by Urrutia and Liñán [10] while higher-order approximations were obtained by Vega [11]. Multiple solutions were also investigated by Cohen [7] for tubular chemical reactors. Tubular reactors are governed by equations that are somewhat more general than those under consideration here. Cohen's approach, however, was different in that his asymptotic analysis was based upon the limit of large diffusion coefficients. Also, his treatment corresponded to the infinite slab geometry.

In the context of elastic membranes, response curves exhibiting multiple solutions were studied by Callegari, Reiss and Keller [8] and by Bauer, Callegari and Reiss [9].

**2. Spherically symmetric formulation.** The spherically symmetric formulation of (1.1) is

$$y''+2x^{-1}y'=F(y)\equiv-\lambda^2(1+\beta-y)\exp[\gamma(y-1)/y], \qquad 0<x<1, \tag{2.1}$$

$$y'(0)=0, \tag{2.2a}$$

$$y(1)=1, \tag{2.2b}$$

where $x$ is the radial coordinate. It can be shown that $y(x)$ is a monotonically decreasing function and that $1<y(x)<1+\beta$. Treating $\beta$ to be a fixed $O(1)$ parameter, we seek the asymptotic expansions of the solutions in the limit $\gamma\to\infty$. Of particular interest is the response curve of the system, i.e. a slice of the $y(0)-\lambda-\gamma$ surface for large $\gamma$.

We shall see that the response curve consists of four distinct parts: the lower oscillatory segment $L_1$, the middle branch $M$, the upper oscillatory segment $L_2$ and the

explosion branch $E$(see Fig. 2). The key to the analysis is the assumption that on each segment, $\lambda$ and $\gamma$ are related in a special way via the expression

$$\lambda^2 = f(\gamma)\exp[-\gamma + \gamma/y_c] \tag{2.3}$$

where $y_c$ is a characteristic temperature and $f(\gamma)$ is at most algebraic in $\gamma$ for large $\gamma$. Both $f(\gamma)$ and $y_c$ may vary from one part of the response curve to the other, but are selected such that all the parts merge together smoothly. With $\lambda$ specified by (2.3), the chemical term $F(y)$ in (2.1) reduces to

$$F(y) = -(1+\beta-y)f(\gamma)\exp[\gamma(y-y_c)/(yy_c)]$$

and the following possibilities arise in the limit $\gamma \to \infty$. When $y(x) < y_c$, $F(y)$ is exponentially small (frozen chemistry). When $y(x) > y_c$, the exponential factor in $F(y)$ is large, forcing $1+\beta-y$ to be exponentially small (chemical equilibrium). Thus $F(y)$ is

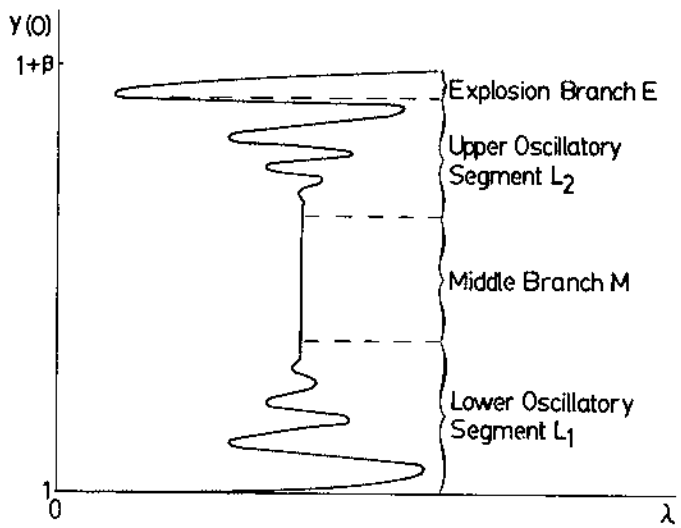


FIG. 2. *The various segments of the response curve for the sphere, for large* $\gamma$.

negligible again, except perhaps in thin layers where large gradients may occur. The chemical term is important only when $y(x) - y_c = O(\gamma^{-1})$, and this may occur either in thin zones or throughout the region.

We shall find that on $L_1$, $y(x) - 1 = o(1)$ throughout the domain. The same is true on $M$ and $L_2$, except that a thin boundary layer (or reaction zone) exists at $x = 0$ in which $y$ undergoes an $O(1)$ variation. On $E$, the thin layer appears in the interior of the domain, separating a frozen region from an equilibrium region. Within this layer the variation of $y$ is $o(1)$.

**3. Lower oscillatory segment $L_1$.** The analysis described below is similar to that appearing in § 3 of [5], but the results are strikingly different.

For $\lambda = 0$, (2.1)–(2.2) have an exact solution $y = 1$. We now perturb about this state, and with $y_c = 1$ in (2.3), seek the expansions

$$\lambda^2 = \Lambda_1(\beta\gamma)^{-1}[1 + \gamma^{-1}\Lambda_2 + \cdots], \tag{3.1}$$

$$y = 1 + \gamma^{-1}y_1 + \gamma^{-2}y_2 + \cdots. \tag{3.2}$$

When (3.1)–(3.2) are inserted into the equations (2.1)–(2.2) and the coefficient of each

negative power of $\gamma$ set to zero, a recursive sequence of problems results. The leading one is

$$y_1'' + 2x^{-1}y_1' = -\Lambda_1 e^{y_1}, \qquad 0 < x < 1, \qquad y_1'(0) = y_1(1) = 0. \tag{3.3}$$

Such a problem was first considered by Emden [12] in connection with isothermal equilibrium of gas spheres, and then by Frank-Kamenetskii [13] to describe thermal ignition of reactive materials. Since then it has been treated by several investigators, including Chandrasekhar and Wares [14], Gelfand [15] and Steggerda [16]. In particular, Gelfand points out that the general solution of (3.3) is given by

$$y_1(x) = y_1(0) + \psi(\alpha x)$$

where $\psi(\xi)$ is the unique solution to the canonical initial-value problem

$$\psi'' + 2\xi^{-1}\psi' = -2e^{\psi}, \qquad 0 < \xi < \infty, \qquad \psi(0) = \psi'(0) = 0 \tag{3.4}$$

and $\alpha$ and $y_1(0)$ satisfy the conditions

$$y_1(0) + \psi(\alpha) = 0, \qquad \alpha = (\Lambda_1/2)^{1/2} \exp[y_1(0)/2]. \tag{3.5}$$

Figure 3 shows the graph of $\psi(\xi)$, obtained numerically. The asymptotic behavior of $\psi$ can be shown to be

$$\psi \sim -2 \ln \xi + A\xi^{-1/2} \sin[\sqrt{7}/2 \ln \xi + B] \quad \text{as } \xi \to \infty, \tag{3.6}$$

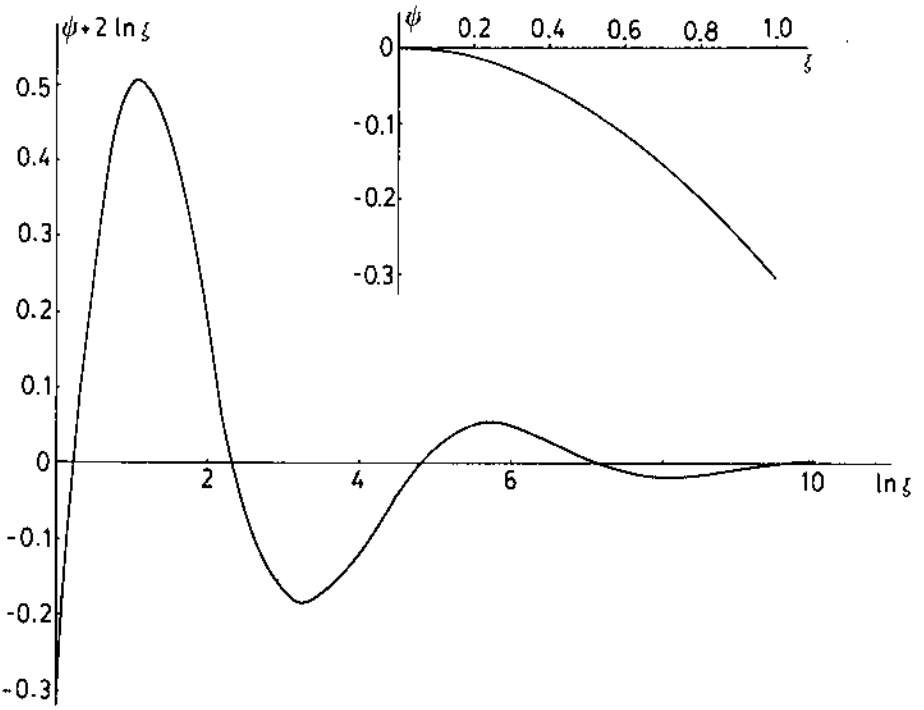


FIG. 3. *Graph of $\psi(\xi)$, the solution of* (3.4). *The main diagram corresponds to $\xi > 1$, and the inset to $0 \leqq \xi \leqq 1$.*

where $A$ and $B$ are known constants. With $\psi$ known, the relations (3.5) yield the dependence of $y_1(0)$ on $\Lambda_1$, graphed in Fig. 4. The graph shows that $y_1(0)$ exists only for $\Lambda_1 < 3.322$, and is then multivalued. There is a decaying oscillation about the asymptote

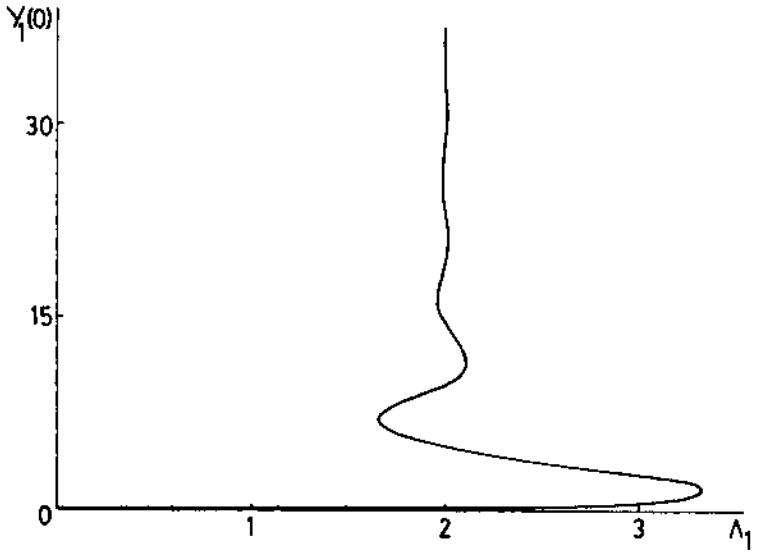


FIG. 4. *Graph of* $\Lambda_1$ *against* $y_1(0)$, *based upon* (3.4).

$\Lambda_1 = 2$, indicating that the number of solutions will be arbitrarily large if $\Lambda_1$ is close enough to 2. (Steggerda [16] has given the coordinates of the first eight turning points of the graph.) In the original variables $\lambda$ and $y(0)$ this graph represents, to leading order, the segment $L_1$ of Fig. 2. On setting $\Lambda_1 = 3.322$ in (3.1) the upper multiplicity bound (or the so-called ignition limit) is given by

$$\lambda^0 = [3.322/(\beta\gamma)]^{1/2}[1 + O(\gamma^{-1})]. \tag{3.7}$$

Higher approximations[1] to this result may be calculated systematically by the procedures outlined in [5], [11] and [17].

The asymptotics (3.2) will breakdown when $y_1(0)$ becomes unbounded, and this occurs as the curve in Fig. 4 approaches the asymptote $\Lambda_1 = 2$, i.e. as one ascends the segment $L_1$ toward the middle branch $M$. The latter corresponds to a different type of solution, to be discussed below.

**4. Middle branch *M*.** On the middle branch the solution is expected to satisfy

$$y(0) = y_*, \qquad 1 < y_* < 1 + \beta. \tag{4.1}$$

We treat $y_*$ as a parameter on $M$, and seek to determine $\lambda$ for which (2.1), (2.2) and (4.1) have a solution. The manner in which the $L_1$-solution developed above broke down ($\Lambda_1 \to 2$) suggests that $\lambda$ assumes approximately the value $\sqrt{2/(\beta\gamma)}$ at the lower end of $M$. However, the analysis of this section will show that to leading order, $\lambda$ retains this value on the *entire* middle branch, i.e. this branch appears as a vertical line on the $y(0)$ versus $\lambda$ plot. This behavior is in contrast to the response of the cylinder or slab [5], where the middle branch has a negative slope. This dissimilarity also extends to the form of the solution $y(x)$. We shall show that it now consists of three separate parts (rather than the two in [5]): an outer solution occupying the bulk of the domain where $y \sim 1$, a relatively thick boundary layer at $x = 0$ in which $y$ rises to $y_*$, and a thin inner boundary

[1] The higher-order terms $y_i$ ($i \geq 2$) of the expansion (3.1) will not, in general, lead to canonical forms similar to (3.4). However, Vega [11] has shown how (3.1) can be replaced by an equivalent expansion whose higher-order terms do lead to canonical equations. Also see [17].

layer which adjusts the slope to comply with the boundary condition $y'(0)=0$. These three solutions are described in §§ 4.1 to 4.3 below, while § 4.4 deals with a modification of the inner solution needed near the upper end of the middle branch.

**4.1. Outer expansion.** On $M$, the expansion for $\lambda$ and the outer expansion for $y$ are taken to be of the same form as (3.1) and (3.2), respectively, with the provision that $\Lambda_1=2$ in (3.1). For the sake of clarity, these expansions are rewritten as

$$\lambda^2=2(\beta\gamma)^{-1}[1+\gamma^{-1}\tilde{\Lambda}_2+\cdots], \tag{4.2}$$

$$y=1+\gamma^{-1}\tilde{y}_1+\gamma^{-2}\tilde{y}_2+\cdots. \tag{4.3}$$

Now, (4.3) is subject to the boundary condition (2.2b) and a matching condition as $x\to 0$. The latter is provided by an intermediate expansion, which will be developed shortly. Thus the leading-order perturbation $\tilde{y}_1$ is found to satisfy

$$\tilde{y}_1''+2x^{-1}\tilde{y}_1'=-2e^{\tilde{y}_1}, \qquad 0<x<1, \qquad \tilde{y}_1(0)=\infty, \qquad \tilde{y}_1(1)=0. \tag{4.4}$$

The matching condition at $x=0$ can be anticipated by recognizing that the perturbation of unity in (4.3) must become positively unbounded, as $x\to 0$, if the solution is to satisfy (4.1), because $y_*=1+O(1)$. As shown in Appendix A, the only solution of (4.4) is

$$\tilde{y}_1=-2\ln x. \tag{4.5}$$

The problem for $\tilde{y}_2$ is found to be

$$\tilde{y}_2''+2x^{-1}\tilde{y}_2'+2e^{\tilde{y}_1}\tilde{y}_2=-2e^{\tilde{y}_1}(\tilde{\Lambda}_2-\tilde{y}_1^2-\tilde{y}_1/\beta), \qquad 0<x<1,$$

$$\tilde{y}_2(0)=\infty, \qquad \tilde{y}_2(1)=0,$$

which, upon substitution for $\tilde{y}_1$ from (4.5), can be solved to yield

$$\begin{aligned}\tilde{y}_2=&\,4(\ln x)^2-(4+2/\beta)\ln x-(\tilde{\Lambda}_2+2-1/\beta)\\&+A_1x^{-1/2}\sin\{(\sqrt{7}/2)\ln x+B_1\},\end{aligned} \tag{4.6}$$

where the constants $A_1$ and $B_1$, yet undetermined, are related by the expression

$$A_1\sin B_1=\tilde{\Lambda}_2+2-1/\beta. \tag{4.7}$$

Higher-order terms in the outer expansion can be developed in a similar way.

**4.2. Intermediate expansion.** In the outer expansion (4.3) the second term assumes the same order as the first when $\ln x=O(\gamma)$, signaling a breakdown. This suggests the nonlinear stretching

$$\ln x=\gamma\sigma \tag{4.8}$$

which reduces (2.1) to

$$dy/d\sigma+\gamma^{-1}d^2y/d\sigma^2=-\lambda^2\gamma(1+\beta-y)\exp[\gamma(1+2\sigma-y^{-1})], \qquad \sigma_0<\sigma<0, \tag{4.9}$$

where $\sigma_0$ will be defined shortly. The argument of the exponent in the above equation now suggests the intermediate expansion

$$y=(1+2\sigma)^{-1}+\gamma^{-1}F_1(\sigma)+\gamma^{-2}F_2(\sigma)+\cdots \tag{4.10}$$

which, when substituted along with (4.2) into (4.9), shows that the $F_i(\sigma)$ can be obtained by simple algebra. In particular, we find that

$$F_1(\sigma)=-(1+2\sigma)^{-2}\ln[\{(1+\beta)(1+2\sigma)^2-(1+2\sigma)\}/\beta]. \tag{4.11}$$

The matching of expansions (4.3) and (4.10) shows that the constant $A_1$ appearing in (4.7) must vanish, since it multiplies a term that is too large in the intermediate region to be matchable. Thus

$$A_1 = 0$$

whence (4.7) yields

$$\tilde{\Lambda}_2 = -2 + 1/\beta.$$

This last result, when substituted into (4.2), reveals that to second order $\lambda$ is independent of $y_*$. In fact it is not difficult to show, via higher-order matching, that $\lambda$ is independent of $y_*$ to all algebraic order in $\gamma$. The middle branch of the response curve is therefore a vertical line.

**4.3. Inner expansion.** The inner boundary conditions $y = y_*$ and $dy/dx = 0$ at $x = 0$ still remain to be satisfied. From (4.10) $y$ equals $y_*$, to leading order, at $\sigma = \sigma_0$ where

$$\sigma_0 = -(y_* - 1)/(2y_*).$$

In order to satisfy the slope condition we need another stretching, given by

$$\sigma = \sigma_0 + \gamma^{-1} \ln(\kappa\rho) \tag{4.12}$$

or, equivalently, by

$$x = \kappa \exp[-\gamma(y_* - 1)/(2y_*)]\rho, \tag{4.13}$$

where $\kappa$ is an $O(1)$ constant, selected to be

$$\kappa = [\beta y_*^2/(1 + \beta - y_*)]^{1/2} \tag{4.14}$$

to keep subsequent algebra simple. The stretchings (4.8) and (4.13) show that the region where $\rho = O(1)$ is a thinner boundary layer, nesting within the region where $\sigma_0 < \sigma < 0$. Upon substitution into (2.1), (4.13) leads to

$$d^2y/d\rho^2 + 2\rho^{-1}\, dy/d\rho = -\lambda^2\kappa^2(1 + \beta - y) \exp[\gamma(y_*^{-1} - y^{-1})], \qquad 0 < \rho < \infty, \tag{4.15}$$

suggesting the inner expansion

$$y = y_* + y_*^2\gamma^{-1}z_1(\rho) + y_*^4\gamma^{-2}z_2(\rho) + \cdots, \tag{4.16}$$

the initial conditions being

$$z_i'(0) = z_i(0) = 0; \qquad i = 1, 2, 3, \cdots. \tag{4.17}$$

The equations for the $z_i$ can be found by substituting (4.2) and (4.16) into (4.15) and equating like powers of $\gamma^{-1}$. The first of these equations is

$$z_1'' + 2\rho^{-1}z_1' = -2e^{z_1}, \qquad 0 < \rho < \infty,$$

which, under initial condition (4.7), constitutes precisely the problem posed by (3.4). The solution, already found, is monotonically decreasing and has the asymptotic behavior

$$z_1 \sim -2 \ln \rho + A\rho^{-1/2} \sin[(\sqrt{7}/2) \ln \rho + B] \quad \text{as } \rho \to \infty.$$

The higher order $z_i$ are found to satisfy linear equations which can also be solved numerically under the initial conditions (4.17).

It can be shown in a straightforward manner that the intermediate expansion (4.10) matches automatically with the inner expansion (4.16). This is to be expected, since the

intermediate solution, to the order considered, does not contain any arbitrary constants still to be determined.

**4.4. Modified inner expansion.** At the upper end of the middle branch, $y_* \to 1+\beta$, causing the constant $\kappa$ in (4.14) to become unbounded, thereby leading to a breakdown of the inner expansion (4.16) developed above. The outer and intermediate expansions are not affected so that only the inner analysis needs to be modified to remedy the situation. Rather than (4.12)–(4.13), the inner stretching is now chosen to be

$$x = \bar{\kappa} \exp[-\gamma\beta/\{2(1+\beta)\}]\bar{\rho}$$

or equivalently,

$$\sigma = -\beta/\{2(1+\beta)\} + \gamma^{-1} \ln(\bar{\kappa}\bar{\rho})$$

where

$$\bar{\kappa} = (\gamma\beta)^{1/2}.$$

We shall show that the middle branch stays vertical even when

$$1+\beta-y(0) = o(1).$$

Let

$$y(0) = 1+\beta-\varepsilon\bar{z}_0, \tag{4.18}$$

where $\bar{z}_0$ is $O(1)$ and positive, and let the solution be expanded as

$$y = 1+\beta+\varepsilon\bar{z}_1(\bar{\rho})+\varepsilon^2\bar{z}_2(\bar{\rho})+\cdots, \tag{4.19}$$

with initial conditions

$$\bar{z}_1(0) = -\bar{z}_0, \quad \bar{z}_1'(0) = 0; \quad \bar{z}_i(0) = \bar{z}_i'(0) = 0 \quad \text{for } i = 2, 3, \cdots. \tag{4.20}$$

Here

$$\varepsilon = (1+\beta)^2/\gamma. \tag{4.21}$$

Proceeding as in § 4.3 above the new leading order inner equation is

$$\bar{z}_1'' + 2\bar{\rho}^{-1}\bar{z}_1' = 2\bar{z}_1 e^{\bar{z}_1}, \qquad 0 < \bar{\rho} < \infty. \tag{4.22}$$

Under the initial conditions (4.20) the solution can only be found numerically but its asymptotic behavior is readily seen to be

$$y(0) = 1+\beta-(\varepsilon/\mu)\exp(-\sqrt{2}/\mu) \tag{4.24}$$

The inner expansion (4.19) now matches the intermediate expansion (4.10); thereby completing the solution.

The above analysis fails when $\bar{z}_0 = o(1)$ because (4.22) then has the solution $\bar{z}_1 \equiv 0$ and (4.23) is not obtained. It can then be shown that the middle branch $M$ stays vertical even when

$$y(0) = 1+\beta-(\varepsilon/\mu)\exp(-\sqrt{2}/\mu) \tag{4.24}$$

where

$$\gamma^{-1} \ll \mu(\gamma) \ll 1. \tag{4.25}$$

(Equation (4.18) above corresponds to $\mu = O(1)$.) The analysis supporting the above assertion is relegated to Appendix B. Even there the description is brief, because the arguments follow rather closely those in the following section.

**5. Upper oscillatory segment $L_2$.** This segment corresponds to $\mu = O(\gamma^{-1})$ in (4.24). We let

$$y(0) = 1 + \beta - a \exp[-\beta/(\sqrt{2}\varepsilon)] \tag{5.1}$$

where $\varepsilon$ is still defined by (4.21) and the positive $O(1)$ parameter $a$ measures the proximity of $y(0)$ to $1+\beta$ on an exponentially small scale. We seek to relate $a$ to $\lambda$, to leading order only, such that the system (2.1), (2.2) and (5.1) has a solution. The leading term in the expansion for $\lambda$ is again of the same form as in (3.1), i.e. we let

$$\lambda^2 = \hat{\Lambda}_1(\beta\gamma)^{-1}[1 + o(\varepsilon)] \tag{5.2}$$

where we stress that $\hat{\Lambda}_1 \not\equiv 2$. An inner region $x = o(1)$ and an outer region $0 < x \leqq 1$ need to be considered. The inner region is further divided into three subregions, and we treat each in turn.

**5.1. Subregion I.** Let

$$x = \delta\hat{\rho},$$

where

$$\delta = [2\gamma\beta/\hat{\Lambda}_1]^{1/2} \exp[-\gamma\beta/(2+2\beta)]. \tag{5.3}$$

This reduces (2.1) to

$$y'' + 2\hat{\rho}^{-1}y' = -2[1 + o(\varepsilon)](1 + \beta - y) \exp[\gamma/(1+\beta) - \gamma/y]. \tag{5.4}$$

The solution $y(\hat{\rho})$ is assumed to have the expansion

$$y = 1 + \beta + \exp[-\beta/(\sqrt{2}\varepsilon)]w_1(\hat{\rho}) + \cdots. \tag{5.5}$$

When substituted into (5.4), (2.2a) and (5.1), the above expansion yields the leading-order problem

$$w_1'' + 2\hat{\rho}^{-1}w_1' = 2w_1, \qquad w_1(0) = -a, \qquad w_1'(0) = 0$$

which has the solution

$$w_1 = -a\{\sinh(\sqrt{2}\hat{\rho})\}/(\sqrt{2}\hat{\rho}).$$

As $\hat{\rho} \to \infty$, $w_1$ becomes exponentially large, signaling a breakdown of the expansion (5.5). This takes us into subregion II.

**5.2. Subregion II.** Here the appropriate independent variable is $\hat{\xi}$, defined by

$$\hat{\rho} = \beta/(2\varepsilon) + \hat{\xi},$$

and we set

$$y = 1 + \beta + \varepsilon v(\hat{\xi}; \varepsilon), \tag{5.6}$$

which reduces (5.4), in the limit $\varepsilon \to 0$, to

$$d^2v/d\hat{\xi}^2 + 4\varepsilon(\beta + 2\varepsilon\hat{\xi})^{-1} dv/d\hat{\xi} = 2v \exp[v - \varepsilon(1+\beta)^{-1}v^2 + \cdots]. \tag{5.7}$$

We shall need a two-term expansion for $v$. This is obtained most conveniently by transferring to the $pv$-plane, where

$$p(v) = dv/d\hat{\xi}. \tag{5.8}$$

Equation (5.7) now reads

$$p\,dp/dv + (4\varepsilon/\beta)(1 + \cdots)p = 2ve^v[1 - \varepsilon(1+\beta)^{-1}v^2 + \cdots], \tag{5.9}$$

and we anticipate, via matching with subregion I, that

$$p(0)=0. \tag{5.10}$$

Now, if $p$ is expanded as

$$p=p_0(v)+\varepsilon p_1(v)+\cdots \tag{5.11}$$

equations (5.9) and (5.10) yield, upon integration, the expressions

$$p_0=-2f(v),$$

$$p_1=[-2f(v)]^{-1}\left[\frac{8}{\beta}\int_0^v f(x)\,dx-\frac{2}{1+\beta}\int_0^v x^3\,e^x\,dx\right],$$

where

$$f(x)\equiv[1+(x-1)e^x]^{1/2}. \tag{5.12}$$

With the two-term expansion (5.11) for $p\equiv dv/d\hat{\xi}$ now known, it is a simple matter to extract the two-term expansion for $v(\hat{\xi};\varepsilon)$. This is is done by substituting

$$v=v_1(\hat{\xi})+\varepsilon v_2(\hat{\xi})+\cdots \tag{5.13}$$

into the implicit expressions (5.11) and performing a single integration, leading to

$$\int_{-1}^{v_1}\frac{x}{f(x)}\,dx=-2(\hat{\xi}-\hat{\xi}_0) \tag{5.14}$$

and

$$v_2=-\tfrac{1}{2}\sqrt{f(v_1)}\int_{-1}^{v_1}\{f(y)\}^{-3/2}\left\{\frac{8}{\beta}\int_0^y f(x)\,dx-\frac{2}{1+\beta}\int_0^y x^3e^x\,dx\right\}dy+\alpha_0\sqrt{f(v_1)}. \tag{5.15}$$

Here, $\hat{\xi}_0$ and $\alpha_0$ are constants of integration; we shall need to determine only $\hat{\xi}_0$ for our purposes. From (5.14) it can be shown that

$$v_1=-\exp\,(I-\sqrt{2}\hat{\xi}_0)\,e^{\sqrt{2}\hat{\xi}}+O(e^{2\sqrt{2}\hat{\xi}})\quad\text{as }\hat{\xi}\to-\infty.$$

This asymptotic result allows the subregion II-expansion (5.6) to match with the subregion I-expansion (5.5), whence

$$\hat{\xi}_0=2^{-1/2}[I+\ln(\sqrt{2}\beta)-\ln a], \tag{5.16}$$

where

$$I=2^{-1/2}\int_{-1}^{0}[\{f(x)\}^{-1}+\sqrt{2}/x]\,dx=0.354. \tag{5.17}$$

Thus $\hat{\xi}_0$ is determined in terms of $a$.

Equations (5.14) and (5.15) also show that

$$\begin{aligned} v_1&=-2\hat{\xi}+\alpha_1+\text{exp small terms},\\ v_2&=4\hat{\xi}^2/\beta+\alpha_2\hat{\xi}+O(1),\quad\text{as }\hat{\xi}\to\infty. \end{aligned} \tag{5.18}$$

Here,

$$\alpha_1=1+2\hat{\xi}_0-J,\qquad \alpha_2=6/(1+\beta)-4(\alpha_1+K)/\beta, \tag{5.19}$$

where

$$J = \int_{-1}^{-\infty} [\{f(x)\}^{-1} - 1]\, dx = -0{\cdot}869, \tag{5.20}$$

$$K = \int_{0}^{-\infty} [f(x) - 1]\, dx = 1.344. \tag{5.21}$$

The asymptotic results (5.18) indicate that the subregion II-expansion (5.6) becomes invalid when $\hat{\xi} = O(\varepsilon^{-1})$, taking us into subregion III.

**5.3. Subregion III.** Here the new independent variable $\hat{\eta}$ is defined by

$$\hat{\eta} = \beta/2 + \varepsilon\hat{\xi}$$

or, equivalently, by

$$\hat{\eta} = \varepsilon\hat{\rho}$$

whence (5.4) reduces to

$$y'' + 2\hat{\eta}^{-1}y' = -2\varepsilon^{-2}[1 + o(\varepsilon)] \exp[\gamma/(1+\beta) - \gamma/y]. \tag{5.22}$$

We anticipate that

$$y < 1 + \beta$$

which further reduces (5.22) to

$$y'' + 2\hat{\eta}^{-1}y' = 0 \quad \text{to all algebraic orders in } \varepsilon. \tag{5.23}$$

The above equation has the general solution

$$y = (K_0 + \varepsilon K_1 + \cdots) + (L_0 + \varepsilon L_1 + \cdots)\hat{\eta}^{-1}. \tag{5.24}$$

Matching with the subregion II-expansion (5.6) yields

$$K_0 = 1, \qquad K_1 = \alpha_1 + \beta\alpha_2/2, \qquad L_0 = \beta^2/2, \qquad L_1 = -\beta^2\alpha_2/4 \tag{5.25}$$

where $\alpha_1, \alpha_2$ are already known (cf. (5.19) above).

The expansion (5.24) itself breaks down in the outer region, where $\hat{\eta}$ is exponentially large, because the RHS of (5.22) is then no longer negligible when compared to the LHS.

**5.4. Outer region.** Here the appropriate independent variable is $x$ itself. The expansion for $y$ is taken as

$$y = 1 + \gamma^{-1}\hat{y}_1(x) + \cdots. \tag{5.26}$$

On substituting (5.2) and (5.26) into (2.1), $\hat{y}_1$ is found to satisfy

$$\hat{y}_1'' + 2x^{-1}\hat{y}_1' = \Lambda_1 e^{\hat{y}_1}, \qquad 0 < x < 1, \tag{5.27}$$

and (2.2b) provides the outer boundary condition

$$\hat{y}_1(1) = 0. \tag{5.28a}$$

Matching of (5.26) with the subregion III-expansion requires that

$$\hat{y}_1'(0) = 0 \tag{5.28b}$$

$$\hat{y}_1(0) = (1+\beta)^2 K_1. \tag{5.29}$$

We note that the problem posed by (5.27) and (5.28) is precisely that appearing in (3.3). Thus the graph of Fig. 4 is again valid, provided the ordinate there is read as $\hat{y}_1(0)$ and the abscissa as $\hat{\Lambda}_1$. We recall that $\hat{\Lambda}_1$ is a factor in the leading term of the expansion (5.2) for $\lambda$. Also, the relation (5.29) can be rewritten as

$$a = \exp\left[\frac{\hat{y}_1(0)}{\sqrt{2}(1+\beta)^2} - \alpha\right], \tag{5.30}$$

once the known value of $K_1$ is substituted from (5.25). In the above expression,

$$\alpha = 2^{-1/2}\left[\frac{2\beta-1}{1+\beta} - \sqrt{2}\,I + J - 2K - \sqrt{2}\ln(\sqrt{2}\beta)\right]$$

and $I, J, K$ are numerical constants, given by (5.17), (5.20) and (5.21), respectively. Thus the graph of Fig. 4 also represents, to leading order, the relationship of $a$ to $\lambda$, once the coordinate axes are rescaled appropriately. Finally, in view of the relationship (5.1) between $y(0)$ and $a$, we conclude that the graph of Fig. 4, turned upside down and its ordinate rescaled yet again, depicts the variation of $y(0)$ with $\lambda$ (to leading order) on the segment $L_2$ of the response curve (see Fig. 2b). It is worth noting that while $y(0)$ varies through an $O(\gamma^{-1})$ amount on $L_1$ (see (3.2)), it only varies through on exponentially small amount on $L_2$ (see (5.1)). Thus $L_2$ is a vertically compressed mirror image of $L_1$ through a horizontal line.

The above solution is valid for $e^{-\alpha} < a < \infty$. For, as $a \to \infty$, i.e. as we descend $L_2$, (5.30) shows that $\hat{y}_1(0) \to \infty$, so that in Fig. 4, $\hat{\Lambda}_1 \to 2$. Thus $L_2$ merges smoothly into $M$. As $a \to e^{-\alpha}$, (5.30) requires that $\hat{y}_1(0) \to 0$, causing $\hat{\Lambda}_1$ to approach zero in Fig. 4. We are then on the highest branch of $L_2$, moving to the left. With $\hat{\Lambda}_1$ decreasing, (5.3) shows that the thickness $\delta$ of the inner region increases. The solution is then approaching the explosion branch, to which we now turn.

**6. Explosion branch *E*.** The analysis needed here is similar in some respects to that which described the explosion branch in [5]. Once again we look for a solution in which the characteristic temperature is $y_c = 1+\beta$ and in which the region $0 < x < 1$ is divided into three distinct zones: a "dead core" where chemical equilibrium prevails ($y(x) = 1+\beta$), a frozen region ($y(x) < 1+\beta$), and a reaction zone ($y \sim 1+\beta$) separating the two. With $y_c = 1+\beta$ in (2.3), $\lambda$ is expanded as

$$\lambda^2 = (1+\beta)^{-4}\gamma^2 \exp\left[-\gamma\beta/(1+\beta)\right][\Omega_1 + \varepsilon\Omega_2 + \cdots]. \tag{6.1}$$

We seek an outer solution of the form (see Fig. 5)

$$y = \begin{cases} y_E(x;\varepsilon) = 1+\beta, & 0 < x < x_0 \quad \text{(equilibrium region)}; \quad (6.2) \\ y_F(x;\varepsilon) < 1+\beta, & x_0 < x < 1 \quad \text{(frozen region)}, \quad (6.3) \end{cases}$$

where $x_0$, the location of the reaction zone, is yet undetermined. Insertion of the expressions (6.1) and (6.3) into (2.1) leads to the equation

$$y'' + 2x^{-1}y' = -(1+\beta)^{-4}\gamma^2(1+\beta-y)\exp\left[\gamma/(1+\beta) - \gamma/y\right](\Omega_1 + \cdots). \tag{6.4}$$

We note that $y = y_E = 1+\beta$ is an exact solution to this equation, subject to the left boundary condition (2.2a). For $y = y_F$, the limit $\gamma \to \infty$ reduces (6.4), to all algebraic orders in $\varepsilon$, to

$$y_F'' + 2x^{-1}y_F' = 0.$$

Subject to (2.2b), the appropriate solution for $y_F$ turns out to be

$$y_F = 1 + C(1-x)/x$$

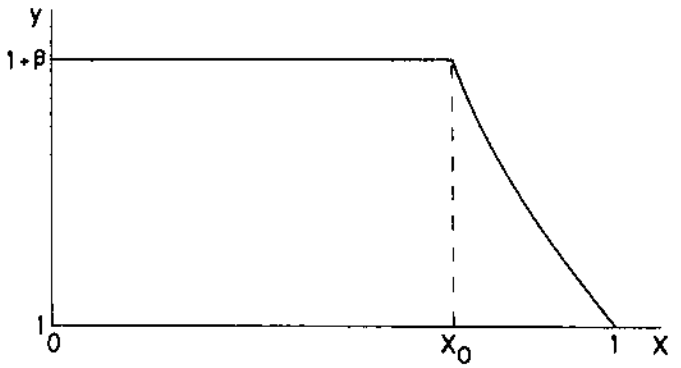


FIG. 5. *Solution profile on the explosion branch.*

where $C$ is determined by the requirement that $y_F$ and $y_E$ be continuous at $x=0$, yielding

$$C = x_0/(1-x_0).$$

The derivatives $y_F'$ and $y_E'$ do not match at $x_0$, requiring a thin "inner" layer for a smooth transition. In this layer we employ the stretching transformation

$$x = x_0 + x_0(1-x_0)\varepsilon\eta \tag{6.5}$$

and seek the expansion

$$y = 1+\beta+\varepsilon\omega_1(\eta)+\cdots. \tag{6.6}$$

When (6.5) and (6.6) are substituted into (6.4), the equation for $\omega_1$ is found to be

$$\omega_1'' = \Omega_1 x_0^2(1-x_0)^2\omega_1\exp(\omega_1), \qquad -\infty<\eta<\infty, \tag{6.7}$$

subject to the boundary conditions

$$\omega_1 = o(1) \quad \text{as } \eta\to-\infty, \qquad \omega_1 = -\beta\eta+o(1) \quad \text{as } \eta\to\infty,$$

which come from matching with the outer solutions $y_F$ and $y_E$. The problem for $\omega_1$ can be completely solved by quadratures, but the result of primary interest is obtained by evaluating the first integral of (6.7) at $\eta=\pm\infty$, yielding

$$\Omega_1 x_0^2(1-x_0)^2 = \beta^2/2. \tag{6.8}$$

The result (6.8), graphed in Fig. 6, determines $\Omega_1$ (and hence $\lambda$; see equation (6.1)) as a function of $x_0$, the location of the reaction zone. It shows that there is a minimum value of $\Omega_1$, corresponding to $x_0=\frac{1}{2}$ and given by

$$\Omega_{1m} = 8\beta^2,$$

such that two values of $x_0$ correspond to each $\Omega_1>\Omega_{1m}$ and none to $\Omega_1<\Omega_{1m}$. Since to leading order $\Omega_1$ is merely a scaled version of $\lambda$ we conclude that there are two solutions or none, according as $\lambda$ is greater than or smaller than the minimum value $\lambda_0$, given by

$$\lambda_0 = \sqrt{8}\gamma\beta(1+\beta)^{-2}\exp[-\gamma\beta/(2(1+\beta))][1+O(\gamma^{-1})], \tag{6.9}$$

obtained by substituting $\Omega_{1m}$ for $\Omega_1$ in (6.1). Thus the analysis yields an explicit asymptotic representation for the lower multiplicity bound $\lambda_0$ and reproduces the upper turn of the response curve. On the $y(0)$ vs. $\lambda$ graph of Fig. 7, based on the above analysis, the two branches coalesce into a single horizontal line because $y(0)=1+\beta$ (to

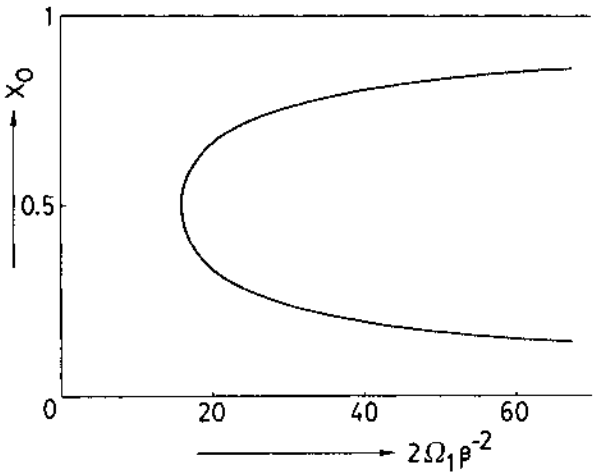


FIG. 6. *Graph of equation* (6.8).

within exponentially small error) for both the solutions under consideration. However, they are drawn distinctly and marked I and II to facilitate identification.

Although the above analysis was based on the tacit assumptions that $x_0$ and $1-x_0$ are both $O(1)$, we now show that the treatment remains valid even when $x_0$ is near the ends of the interval (0, 1). As $x_0 \to 1$, (6.8) shows that $\Omega_1$ becomes large, so that in Fig. 7, $\lambda$ increases on branch *I*. In fact $\lambda$ can increase indefinitely on this branch as $x_0$ gets closer and closer to unity, without violating any aspects of the above analysis. Physically, the entire pellet is now occupied by the dead core, except for a narrow frozen region (of width $1-x_0$) adjacent to the surface. The two regions are separated by an extremely thin (of width $\gamma^{-1}(1-x_0)$) reaction zone.

As $x_0 \to 0$, the frozen region extends toward the center of the pellet, squeezing the reaction zone and the dead core. Equation (6.8) shows that $\Omega_1$ becomes large again, but now $\lambda$ increases on branch II in Fig. 7. However, $x_0$ cannot become too small, i.e. $\lambda$ cannot become too large without restoring the hitherto negligible RHS of (6.4). In that case, the appropriate solution is that corresponding to the branch $L_2$, discussed in § 5 above. A simple perturbation analysis along the lines of that of § 5 yields the next-order approximation to $y(0)$ in the dead core, and shows that the branches $E$ and $L_2$ merge smoothly.

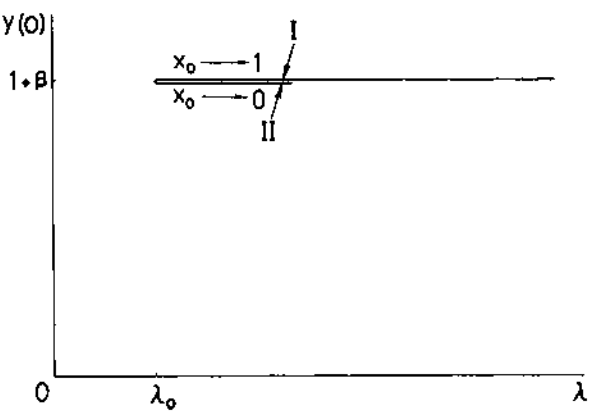


FIG. 7. *The explosion branch E.*

**7. Concluding remarks.** The results obtained above can now be used to construct the response curve of the system, and this has been done in Fig. 8 for $\gamma = 100$ and $\beta = 0.5$. The figure shows a composite curve, formed by the smooth merging into one another of the various segments described above.

Some remarks about the results are in order.

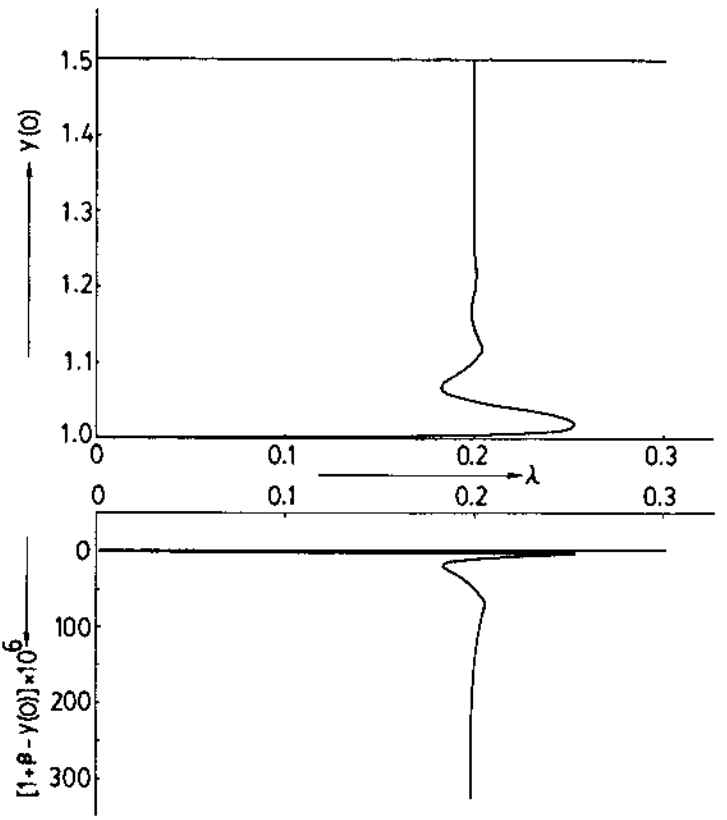


FIG. 8. *The composite response curve for $\gamma = 100$ and $\beta = 0.5$. The upper oscillatory segment, too thin to appear prominently in the upper diagram, is displayed on an expanded scale in the lower diagram.*

(i) Figure 8 shows that the upper oscillatory segment $L_2$ is confined to an extremely narrow band, as compared to the lower oscillatory segment $L_1$. This is because $y(0)$ undergoes an exponentially small variation on $L_2$ but a larger $O(\gamma^{-1})$ variation on $L_1$. However, we note that even on $L_2$, the solution in the outer region $0 < x \leqq 1$ does experience an $O(\gamma^{-1})$ change; see the expansion (5.26). Therefore, if a graph of $\gamma$ were to be plotted against some functional of the outer solution, e.g. the slope $y'(1)$, both oscillatory segments will be displayed equally prominently.

(ii) It is clear that the multiplicity of solutions, which corresponds to the number of intersections of the response curve with the $\lambda$ = constant line, increases as $\lambda$ approaches the asymptotic value $\sqrt{2/(\beta\gamma)}$. Strictly speaking, the number of solutions can be arbitrarily large. In practice, however, the oscillations on both $L_1$ and $L_2$ decay rapidly toward the middle branch. Therefore, only an extremely fine resolution will reveal more than a few solutions, as Copelowitz and Aris [4] discovered through numerical work.

(iii) Our analysis assumes that $\beta$ is a fixed, $O(1)$ parameter. Aris [1] has pointed out that small values of $\beta$ often occur in practice, which suggests that the limit $\beta \to 0$ is

physically significant. It is not difficult to check that our *entire* analysis remains valid for $\beta \to 0$, provided $\gamma\beta \to \infty$.

(iv) Since the multiplicity bounds $\lambda_0$ and $\lambda^0$ are of practical interest, their asymptotic values are plotted against $\gamma$ for various $\beta$ in Figs. 9 and 10. These bounds were also calculated numerically by means of the initial-value technique devised by Weisz and Hicks [18]. Figure 11 shows a comparison of the asymptotic and numerical results for $\beta = 0.5$. At $\gamma = 20$, the error is under five percent for $\lambda_0$ and under fifteen

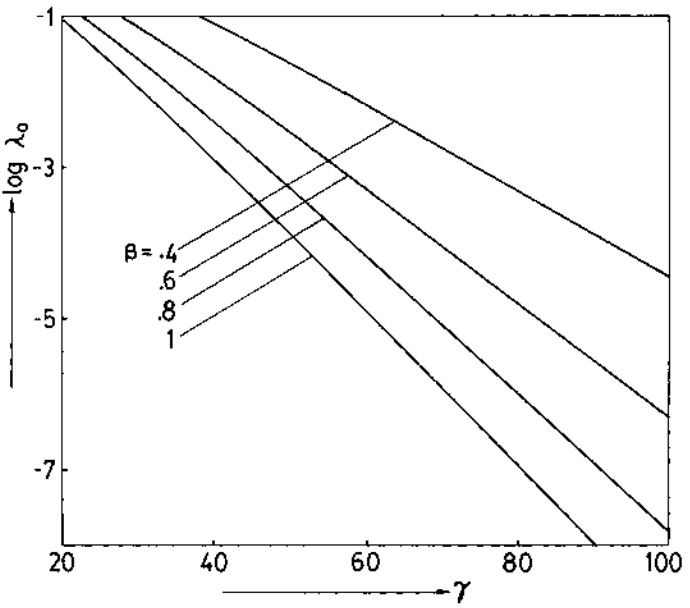


FIG. 9. *Curves of* $\lambda_0$ *versus* $\gamma$ *for* $\beta = 0.4, 0.6, 0.8$ *and* $1.0$ *according to the asymptotic formula* (6.9).

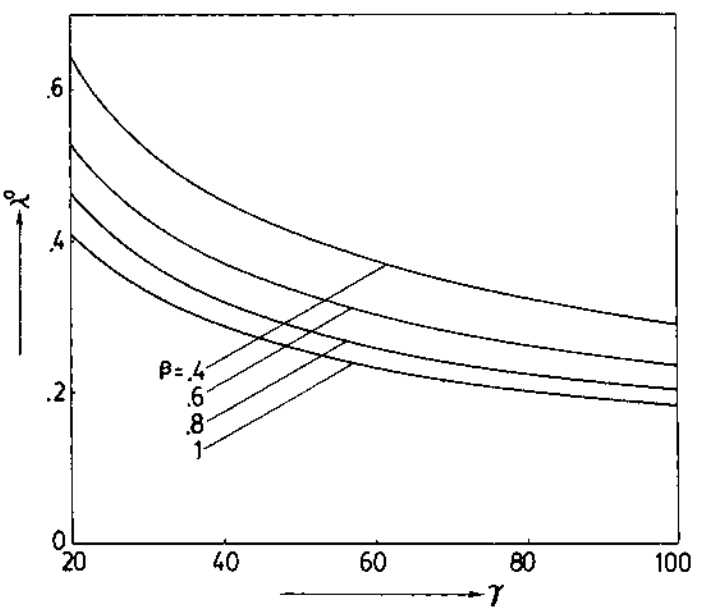


FIG. 10. *Curves of* $\lambda^0$ *versus* $\gamma$ *for* $\beta = 0.4, 0.6, 0.8$ *and* $1.0$ *according to the asymptotic formula* (3.7).

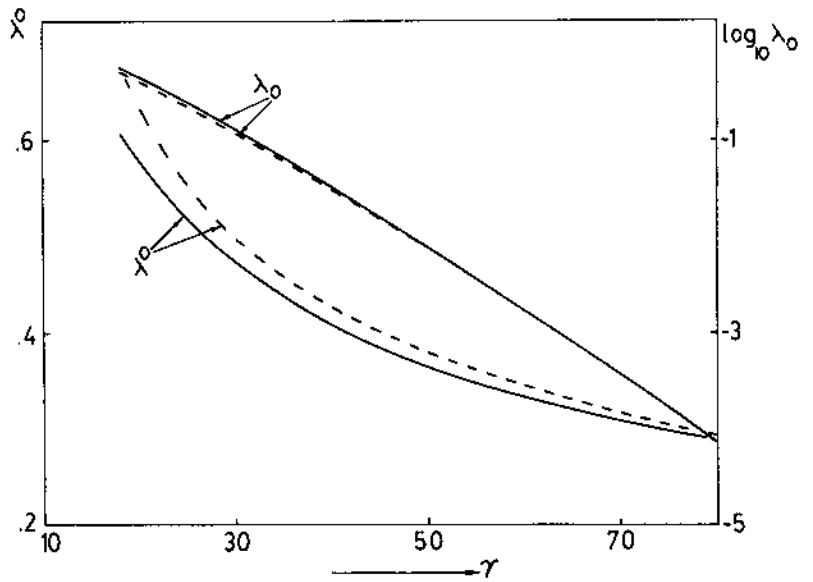


FIG. 11. *Comparison of asymptotic* (———) *and numerical* (– – – –) *results for* $\lambda^0$ *and* $\lambda_0$, *for* $\beta = 0.5$.

percent for $\lambda^0$, and the agreement improves with increasing $\gamma$. Other numerical results not displayed here indicate that for fixed $\gamma$, the error decreases with increasing $\beta$.

(v) Finally, we reiterate a remark made in the Introduction. Even though the static response of the sphere is vastly different from that for the slab or the cylinder, it is conceivable that only the extreme branches of the response curve are stable. Dynamically, therefore, there may be little qualitative difference between the sphere and the other two geometries.

**Appendix A. Analysis of problem (4.4).** Consider the differential equation

$$y'' + 2x^{-1}y' = -2e^y, \qquad 0 < x < 1. \tag{A.1}$$

We now show that of all the solutions of (A.1) that satisfy the condition

$$y(1) = 0, \tag{A.2}$$

the only one that becomes positively unbounded as $x \to 0+$ is the solution

$$y_0(x) = -2 \ln x. \tag{A.3}$$

On writing

$$\ln x = \eta, \qquad y(x) = -2\eta + z(\eta), \tag{A.4}$$

(A.1) reduces to

$$z'' + z' = 2(1 - e^z), \qquad -\infty < \eta < 0, \tag{A.5}$$

which, via the substitutions

$$z = \ln u, \qquad z' = v, \tag{A.6}$$

yields

$$du/d\eta = uv, \qquad dv/d\eta = 2 - 2u - v. \tag{A.7}$$

The phase portrait of the autonomous system (A.7) is drawn in Fig. A.1. There are two critical points: an unstable spiral at (1, 0) and a saddle point at (0, 2). For real $z$, only the right-half phase plane is of interest.

The substitutions (A.4) and (A.6) show that the condition (A.2) reduces to

$$u(0) = 1. \tag{A.8}$$

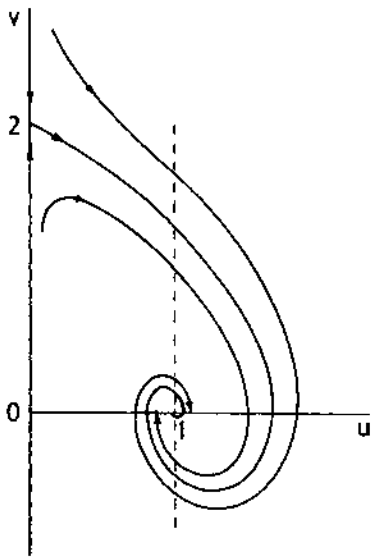


FIG. A.1. *Phase portrait of equations* (A.7).

All the solutions of (A.7) satisfying (A.8) start on the line $u = 1$ in the phase plane. Depending upon the initial value $v(0)$, the solution can behave in three different ways as $\eta \to -\infty$ (i.e. as $x \to 0$):

(i) $u \equiv 1$ and $v \equiv 0$ (i.e. $z \equiv 0$ or $y \equiv y_0(x)$); this corresponds to a start at the critical point (1, 0).

(ii) $u \to 0$ and $v \to 2$; this corresponds to those solutions that lie on the separatrix (excluding (i) above).

(iii) $u \to 0$ and $v \to \pm\infty$; this corresponds to the solutions that do not lie on the separatrix.

Since $u \to 0$ implies $z \to -\infty$, it is easily shown from (A.5) that the cases (ii) and (iii) above, respectively, correspond to

$$z \sim 2\eta + \text{constant} \quad \text{as } \eta \to -\infty$$

and

$$z \sim -Be^{-\eta} + 2\eta + \text{constant} \quad \text{as } \eta \to -\infty \quad (B > 0)$$

or, equivalently, to

$$y \sim \text{constant} \quad \text{as } x \to 0$$

and

$$y \sim -B/x + \text{constant} \quad \text{as } x \to 0.$$

Neither of these two possibilities leads to a positively unbounded solution. That only leaves case (i) above, i.e. the solution $y_0(x)$, as asserted.

**Appendix B. Modified inner expansion near the top end of the middle branch *M*.** We now show that the middle branch remains vertical, to leading order, even when

$$y(0) = 1 + \beta - (\varepsilon/\mu) \exp(-\sqrt{2}/\mu), \tag{B.1}$$

where $\mu$ is a small parameter subject to the restrictions (4.25). As in § 4, the domain splits up into an outer region, an intermediate region and an inner region. The first two regions have the same expansions as before (cf. (4.3) and (4.10)); only the inner analysis requires modification. The inner region, characterized by the independent variable $\bar{\rho}$ (see § 4.4) is further divided into *four* subregions, which we now describe. The description will be brief since part of the analysis follows that of § 5.

In subregion I we assume the expansion

$$y = 1 + \beta(\varepsilon/\mu) \exp(-\sqrt{2}/\mu)\bar{w}_1(\bar{\rho}) + \cdots \tag{B.2}$$

and, following the treatment of § 5.1, it can be shown that

$$\bar{w}_1 = -\{\sinh(\sqrt{2}\,\bar{\rho})\}/(\sqrt{2}\,\bar{\rho}).$$

The exponential behavior of $\bar{w}_1$ for large $\bar{\rho}$ indicates that (B.2) is then invalid.

In subregion II we let

$$\bar{\rho} = \mu^{-1} + \bar{\xi}$$

and seek the expansion

$$y = 1 + \beta + \varepsilon\bar{v}_1(\bar{\xi}) + \cdots. \tag{B.3}$$

The procedure of § 5.3 shows that $\bar{v}_1$ is given by an implicit expression similar to (5.14), and that $\bar{v}_1$ has the asymptotic behavior

$$\bar{v}_1 = -2\bar{\xi} + O(1) \quad \text{as } \bar{\xi} \to \infty.$$

The above result suggests the breakdown of (B.3) for large $\xi$.

In subregion III, the new independent variable $\bar{\eta}$ is defined by

$$\bar{\eta} = 1 + \mu\bar{\xi}$$

and the expansion proceeds as

$$y = 1 + \beta + (\varepsilon/\mu)\bar{\phi}_1(\bar{\eta}) + \cdots. \tag{B.4}$$

It can be shown that $\bar{\phi}_1$ satisfies the chemistry-free equation

$$\bar{\phi}_1'' + 2\bar{\eta}^{-1}\bar{\phi}_1 = 0, \qquad 1 < \bar{\eta} < \infty, \tag{B.5}$$

and matching with (B.3) leads to the solution

$$\bar{\phi}_1 = -2(\bar{\eta} - 1)/\bar{\eta}.$$

As $\bar{\eta} \to \infty$, the chemistry term ignored in the derivation of (B.5) becomes as important as the terms retained there. This puts us in subregion IV, where the independent variable $\bar{\zeta}$ is taken to be

$$\bar{\zeta} = \sqrt{2}\,\mu^{-3/2} \exp(-1/\mu)\bar{\eta}.$$

The solution is expanded as

$$y = 1 + \beta - 2(\varepsilon/\mu) + \varepsilon\bar{\psi}_1(\bar{\zeta}) + \cdots \tag{B.6}$$

and it can be shown that $\bar{\psi}_1$ satisfies

$$\bar{\psi}_1'' + 2\bar{\zeta}^{-1}\psi_1' = -2e^{\bar{\psi}_1}, \qquad 0 < \bar{\zeta} < \infty. \tag{B.7a}$$

Matching with (B.4) provides the boundary conditions

$$\bar{\zeta}_1(0) = \bar{\zeta}_1'(0) = 0. \tag{B.7b}$$

Equations (B.7) pose precisely the same problem as (3.4) whose solution, as indicated by (3.6), has the asymptotic behavior

$$\bar{\psi}_1 \sim -2 \ln \bar{\zeta} + A\bar{\zeta}^{-1/2} \sin[\sqrt{7}/2 \ln \bar{\zeta} + B] \quad \text{as } \bar{\zeta} \to \infty.$$

It is now readily shown that (B.6) matches with the intermediate expansion (4.10), provided $\mu \gg \varepsilon$, and this is where the lower bound restriction on $\mu$ in (4.25) comes into play.

We note that throughout the above analysis,

$$\lambda^2 \sim 2(\beta\gamma)^{-1},$$

(cf. (4.2)), which demonstrates the validity of the assertion made at the beginning of this appendix.

**Acknowledgment.** The authors wish to thank Professor Stuart Hastings who pointed out an omission in an earlier version of the paper.

REFERENCES

[1] R. ARIS, *The Mathematical Theory of Diffusion and Reaction in Permeable Catalysts*, Vol. I, Clarendon Press, Oxford, 1975.

[2] ———, *The Mathematical Theory of diffusion and Reaction in Permeable Catalysts*, Vol. II, Clarendon Press, Oxford, 1975.

[3] M. L. MICHELSON AND J. VILLADSEN, *Diffusion and reaction in spherical catalyst pellets: steady state and local stability analysis*, Chem. Engrg. Sci., 27 (1972), pp. 751–762.

[4] I. COPELOWITZ AND R. ARIS, *Communications on the theory of diffusion and reaction—V. Findings and conjectures concerning the multiplicity of solutions*, Ibid., 25 (1970), pp. 906–909.

[5] A. K. KAPILA AND B. J. MATKOWSKY, *Reactive-diffusive systems with Arrhenius kinetics: multiple solutions, ignition and extinction*, this Journal, 36 (1979), pp. 373–389.

[6] R. JACKSON, *A simple geometric condition for instability in catalyst pellets at unit Lewis number*, Chem. Engrg. Sci., 28 (1973), pp. 1355–1358.

[7] D. S. COHEN, *Multiple solutions of nonlinear partial differential equations*, Nonlinear Problems in the Physical Sciences and Biology, I. Stakgold, D. D. Joseph and D. H. Sattinger, eds., Springer-Verlag, New York, 1973.

[8] A. J. CALLEGARI, E. L. REISS AND H. B. KELLER, *Membrane buckling: a study of solution multiplicity*, Comm. Pure Appl. Math., 24 (1971), pp. 499–516.

[9] L. BAUER, A. J. CALLEGARI AND E. L. REISS, *On the collapse of shallow elastic membranes*, Nonlinear Elasticity, R. W. Dickey, ed., Academic Press, New York, 1973.

[10] J. L. URRUTIA AND A. LIÑÁN, *Steady heat and mass transfer in porous catalyst particles*, Development of an Analytical Model of Hydrazine Decomposition Motors, Instituto Nacional De Tecnica Aerospacial "Esteban Terradas," Estec Contract No. 1121/70 AA, Part III, Madrid, 1975.

[11] J. M. VEGA, *Technicas de perturbaciones en la teoria de reactores cataliticos*, Ph.D. Thesis, E.T.S. de Ingenieros Aeronauticos, Universidad Politechnica de Madrid, Madrid, 1977.

[12] R. EMDEN, *Gaskugeln, Anwendug der mechanischen Warmentheorie auf Kosmologie*, Teubner, Leipzig, 1907.

[13] D. A. FRANK-KAMENETSKII, *Diffusion and Heat Transfer in Chemical Kinetics*, Plenum Press, New York, 1969.

[14] S. CHANDRASEKHAR AND G. W. WARES, *The isothermal function*, Astrophys. J., 109 (1949), pp. 551–562.

[15] I. M. GELFAND, *Some problems in the theory of quasilinear equations*, Trans. Amer. Math. Soc., 2 (1963), pp. 295–381.

[16] J. J. STEGGERDA, *Thermal stability: an extension of Frank-Kamenetskii's theory*, J. Chem. Phys., 43 (1965), pp. 4446–4448.

[17] J. M. VEGA AND A. LIÑÁN, *Regular perturbations of the Frank-Kamanetskii equation: Higher-order approximations of the ignition regime*, 1979, in preparation.

[18] P. B. WEISZ AND J. S. HICKS, *The behavior of porous catalyst particles in view of internal mass and heat diffusion*, Chem. Engrg. Sci., 17 (1962), pp. 265–275.